THE JOURNAL OF PHYSICAL CHEMISTRY A

Article

pubs.acs.org/JPCA

Characterization of Highly Unusual NH^+–O Hydrogen Bonding to Ester Ether Oxygen Atoms through Spectroscopic and Computational Studies

Michael T. Scerba,[†] Andrew F. DeBlase,[‡] Steven Bloom,[†] Travis Dudding,[§] Mark A. Johnson,*[,‡] and Thomas Lectka*[,†]

Contribution from the Departments of Chemistry: [†]New Chemistry Building, Johns Hopkins University, 3400 North Charles Street, Baltimore, Maryland 21218, United States

[‡]Sterling Chemistry Laboratory, Yale University, P.O. Box 208107, New Haven, Connecticut 06520, United States

[§]Brock University, St. Catherines, Ontario L2S 3A1, Canada

Supporting Information

ABSTRACT: We characterize a highly unusual, charged NH–O hydrogen bond formed within esters of 8-(dimethylamino)-naphthalen-1-ol in which an ammonium ion serves as an intramolecular hydrogen bond donor to spatially proximate ester ether oxygen atoms. Infrared spectroscopic analysis of the ester carbonyl frequencies demonstrates significant blue-shifting when ether hydrogen bonding is possible, in stark contrast to the more commonly observed red shift that occurs upon hydrogen bonding to the ester carbonyl oxygen. The intrinsic behavior of the linkage (i.e., in which counterions and solvent effects are eliminated) is provided by vibrational predissociation spectroscopy of the isolated gas-phase cations complexed with weakly bound D_2 molecules.

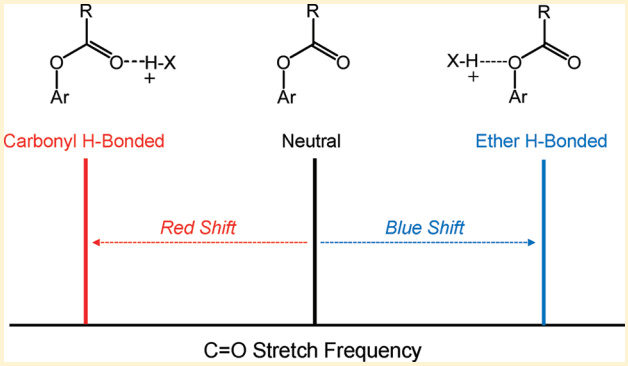

INTRODUCTION

The ability of carboxylic acid esters to accept hydrogen bonds has a profound influence on their reactivity, and the distinct manifolds through which these fundamental interactions operate illustrate the elegant yet complex nature of chemical bonding. While esters contain two electronegative oxygen atoms, it is the highly polarized ester carbonyl oxygen (O_{ester}) that typically engages in hydrogen bonding.[1] Such interactions have a significant impact on biochemical processes relating to the organization of cell membranes,[2,3] the association of sterols to phospholipids,[4] and the conformational preferences of certain amino acid esters.[5] In chemical systems, hydrogen bonds to carbonyl oxygen atoms have been detected in a variety of esters, lactones, amides, and carbonates.[6,7] Similar interactions occur in substituted salicylates[8] and naphthoates,[9] including an impressive nine-membered intramolecular hydrogen bond formed within a (phenoxymethyl)methylnaphthoate derivative.[10] Hydrogen bonding to the ester carbonyl oxygen has even been implicated in asymmetric methods of natural product synthesis.[11]

Perhaps more interesting (and certainly *much* less documented) are cases in which hydrogen bonds are formed preferentially to esters via the alkoxy ether oxygen (O_{ether}). When compared to the carbonyl oxygen, the alkoxy oxygen exhibits weaker proton affinity and therefore should act as a less-suitable hydrogen bond acceptor.[12] However, crystal structures of a variety of enzyme–substrate complexes involving bound esters place the ether oxygen proximal to H-bond donors in contexts including alcohols, primary and secondary amines, and even imino groups.[13] Moreover, discrete ether protonation has been suggested in the $A_{AC}1$-type acid hydrolysis of bulky mesityl esters[14] and during the acid-catalyzed $A_{AL}2$ hydrolysis of select γ-lactones.[15] Despite these examples, there is no direct evidence, to our knowledge, for charged donors providing a hydrogen bond to an ester alkoxy-oxygen in the literature. In this article, we present conclusive spectroscopic and computational evidence for a charged NH–O_{ether} hydrogen bond formed within 1,8-disubstituted naphthalene derivatives.

RESULTS AND DISCUSSION

Our interest in charged, intramolecular hydrogen bonding stems back to work conducted on NHN contacts within (*N*-acyl) Proton Sponge derivatives.[16] Recently, we reported the thorough characterization of a charged NH–F hydrogen bond in a 1,8-disubstituted fluorinated aminonaphthalene.[17] On the basis of these previous efforts, we reasoned that an ammonium ion, appropriately positioned on a disubstituted naphthalene

Received: December 5, 2011
Revised: March 4, 2012
Published: March 6, 2012

   dx.doi.org/10.1021/jp211688v | *J. Phys. Chem. A* 2012, 116, 3556–3560

skeleton, could serve as a scaffold to isolate a charged intramolecular hydrogen bond to an ether oxygen of a carboxylic acid ester, NH−O_{ether} (Figure 1).

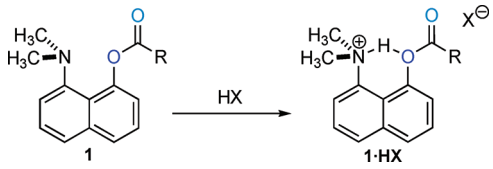

Figure 1. Formation of a charged, intramolecular NH−O_{ether} hydrogen bond.

We first carried out a computational survey of a series of protonated 8-(dimethylamine)naphthalene-1-yl esters **1** and **2** (Figure 2) to evaluate the structural motifs at play. Geometry

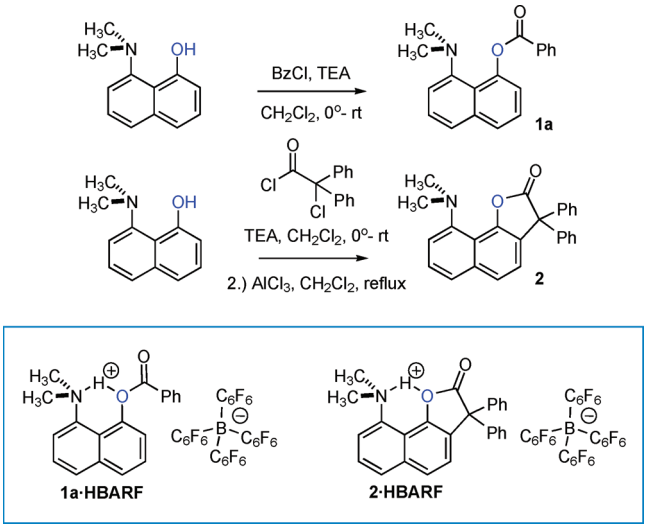

Figure 2. Synthesis of naphthyl esters and ion structures.

optimizations and subsequent vibrational analyses (DFT/B3LYP/6-311++G**) of the corresponding ammonium cations suggest that the low energy structure for **1a**·H^+ includes hydrogen bonding to the ether−ester oxygen. The alternative structure wherein hydrogen bonding occurs to the carbonyl group is about 1.5 kcal·mol^{-1} higher in energy (Supplemental Table 1, Supporting Information). Moreover, lactone **2**, which was made by a simple acylation/Friedel−Crafts sequence, can only yield NH−O_{ether} hydrogen bonds due to geometric constraints.

We anticipate that, whereas H-bonding to the ester carbonyl should induce a red shift of the corresponding C=O stretch, ether−ester H-bonding should reveal a complementary blue shift (Figure 3). This phenomenon can be readily understood by both resonance and orbital arguments. For example, ether−ester H-bonding is expected to disrupt ester resonance by reducing the electron donating capacity of the ether oxygen. Therefore, ether−ester H-bonding should favor the acylium resonance form (Figure 3). From an orbital standpoint, ether−ester H-bonding should decrease the energy of the σ^*(C−O), making it a better energetic match for overlap with $n(O_{ester})$ (a lone pair on the carbonyl oxygen). This effect can also be understood in the context of the gas phase ion chemistry literature,[18] where protonation at the less basic ether position leads to formation of the acylium ion in the proton driven

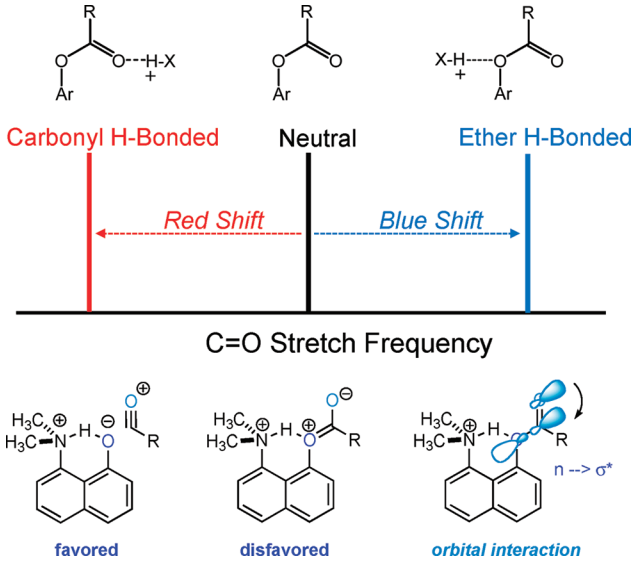

Figure 3. Expected IR shifts and electronic rationalizations.

dissociation of carbonyl compounds such as carboxylic acids,[19,20] esters,[21,22] and α,β-unsaturated ketones.[23]

Such a mechanism for acyl-oxygen fission ($A_{AC}1$)[21] typically takes precedence only at fairly acidic conditions in the condensed phase[24] because protonation of the carbonyl oxygen is thermodynamically more favorable. In compound **1a**·H^+, of course, the ether−ester oxygen is not fully protonated but rather participates in an intramolecular proton bond with the dimethylamino group. Isolation of the H-bonding interaction requires pairing **1a** and **2** with weakly coordinating counterions. Therefore, following protonation with HCl, the chloride counterions were exchanged for the tetrakis(perfluorophenyl) borate ion ($B(C_6F_5)_4^-$). In addition to being weakly coordinated, the $B(C_6F_5)_4^-$ ion usually allows for otherwise poorly soluble ions to dissolve readily in organic solvents.

The neutral forms of ester **1a** and lactone **2** were analyzed by IR spectroscopy in dichloromethane (see Supporting Information) and were observed to display isolated carbonyl resonances, ν_{CO}, at 1735 and 1801 cm^{-1}, respectively (Table 1). The only **1a**·**HB**$(C_6F_5)_4$ and **2**·**HB**$(C_6F_5)_4$ bands in the

Table 1. Summary of Carbonyl Peak Positions in Solution Phase FTIR and Gas Phase D_2 Predissociation Spectra of Cryogenic Ions[a]

	solution phase		cryogenic gas phase (± 5 cm^{-1})
	neutral	·**HB**$(C_6F_5)_4$	·H^+
1a	1735	1771	1792
2	1801	1839	
3	1720[31]		1500−1700[b]

[a]Vibrational frequencies are in cm^{-1}. [b]This range in **3**·H^+ contained many bands associated with carbonyl CO stretching.

carbonyl region appeared significantly blue-shifted from the parent neutral values, appearing at 1771 and 1837 cm^{-1}, respectively. These blue shifts (36 cm^{-1} for **1a**·**HB**$(C_6F_5)_4$ and 38 cm^{-1} for **2**·**HB**$(C_6F_5)_4$) are consistent with the calculated behavior of the NH−O_{ether} interaction (e.g., 31 cm^{-1} at the harmonic level (B3LYP/6-311++G**, scaled by 0.982) for **1a**), and we therefore assign these transitions to the ν_{CO} fundamentals. In each case, no peaks were observed below

dx.doi.org/10.1021/jp211688v | J. Phys. Chem. A 2012, 116, 3556−3560

these ν_{CO} features where we would expect bands from the NH−O_{ester} motif. While this behavior was expected in the conformationally constrained lactone **2·HB(C_6F_5)$_4$** (since it cannot engage in simultaneous hydrogen bonding between R_2NH^+ and the ester carbonyl), the absence of lower energy ν_{CO} bands in **1a·HB(C_6F_5)$_4$** indicates that the higher energy isomer with an H-bond to O_{ester} is not populated at room temperature.

To explore the intrinsic character of the NH−O_{ether} linkage, we also obtained infrared spectra of the isolated, gas phase ions corresponding to **1a·H$^+$** and several related compounds. These spectra were obtained in a mass-selective fashion by monitoring the predissociation of the weakly bound D_2 adducts, prepared using cryogenic ion chemistry.[25] It is possible, of course, that D_2 attachment perturbs the intrinsic spectrum of the ion, but we note that earlier studies of proton-bound binary complexes indicate that Ar and H_2 yield similar bonding energies and attachment sites.[26−28] In the Ar case, (e.g., $(CH_3)_2O$−$H^+O(CH_3)_2$) the tag actually avoids the shared proton and thus yields minimal solvent shift of the bands, while accessible noncomplexed NH and OH sites are red-shifted upon tag attachment (e.g., <15 cm^{-1} in H_2 attachment to an $-NH_3^+$ group).[29] In cases where D_2 is strongly bound (500 cm^{-1}), the H_2 stretch is evident in the spectrum, and the molecules are readily condensed onto the ions in the 10 K trap. In the present case, we therefore expect relatively significant H_2 shifts in the X−H$^+$ stretching bands of the control species **3·H$^+$** and **4·H$^+$** (see top trace in Figure 4), which feature intermolecular proton bonding to the tag, but the main target molecule for this study (**1a·H$^+$**) should be less affected by complex formation. This conclusion is supported by the fact that the H_2 stretch was not observed in the **1a·H$^+$·H_2** complex, and that photodissociation was observed down to 900 cm^{-1} (not shown), giving an upper bound to the D_2 binding energy. Similar systems exhibit binding energies in the 350−500 cm^{-1} range.[29] Finally, we note that the observed spectra were essentially identical for the complexes with one and two H_2 adducts (Supplemental Figure 5, Supporting Information), confirming that the incremental solvent shift is indeed small.

We first establish the frequencies associated with protonation of the two isolated components that are engaged in the intramolecular proton bond in **1a·H$^+$**. This was accomplished by measuring the spectra of the protonated benzoate (**3**, black) and dimethylamino (**4**, blue) derivatives, presented in Figure 4b. Protonation of the amine (**4·H$^+$**) reveals the position of the nonbonded N−H$^+$ stretch through its single isolated, intense transition (blue) at 3265 cm^{-1}. Protonation of 1-naphthylbenzoate (**3·H$^+$**), however, should occur at the more basic carbonyl position, which is not available for intramolecular proton bonding in **1a·H$^+$** due to the constrained geometry required for C=O linkage to the amino group. Like the protonated amine, the **3·H$^+$** spectrum displays a strong, sharp band at 3313 cm^{-1} (teal in Figure 4b) readily assigned to the nonbonded OH stretch. This feature lies 65 cm^{-1} below that reported previously[30] for gas phase, protonated acetone, ν_{OH}^{AcH+} = 3378 cm^{-1}.

Turning to the CO stretching frequency, we note that the **3·H$^+$** spectrum displays many bands in the 1500−1700 cm^{-1} range nominally associated with this functional group, which is consistent with the character of the computed normal modes. In particular, the C=OH$^+$ motif is not predicted to occur as an isolated oscillator but is rather coupled with aromatic CC stretch deformations and the COH bend in the 1450−1650 cm^{-1} range. Thus, the bands consistent with the predicted ν_{CO} activity are bracketed in red in Figure 4b. The calculated pattern is available in Supplemental Figure 1, Supporting Information. Most importantly, *all* these bands are significantly red-shifted relative to the ν_{CO} location in neutral 1-naphtholbenzoate (green arrow at 1720 cm^{-1} in Figure 4b), by a similar amount as that (~150 cm^{-1}) observed by Duncan and co-workers[30] for the case of acetone protonation, where $\nu_{CO}^{AcH^+}$ = 1580 cm^{-1} (dark brown arrow in Figure 4b).

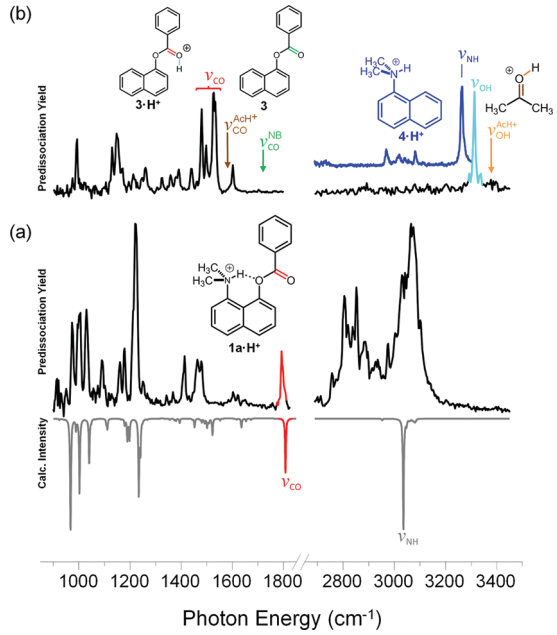

Figure 4. Vibrational predissociation spectra of the D_2 tagged, gas phase ions of (a) **1a·H$^+$** and the model compounds (b) **3·H$^+$** (black trace) and **4·H$^+$** (blue trace). The inverted spectrum in the lower trace presents the calculated harmonic spectrum of isolated **1a·H$^+$** ions obtained at the B3LYP/6-311++G** level of theory using the following scaling factors: 0−1750 cm^{-1} = 1.00, C=O stretching = 0.982, C−H stretching = 0.961, and N−H stretching = 0.945. In each spectrum, the carbonyl resonance is colored in red. Arrows indicate the carbonyl and OH vibrations of argon-tagged protonated acetone[30] (ν_{CO}^{AcH+} and ν_{OH}^{AcH+}, respectively), and the carbonyl stretch (ν_{CO}^{NB}) in neutral 1-naphthylbenzoate (NB, **3**).[31] Peaks/arrows are color-coded according to the bond displacements that contribute most to the calculated normal mode at the corresponding frequency.

Figure 4a presents the **1a·H$^+$** predissociation spectrum along with that calculated (B3LYP/6-311++G**) at the harmonic level, displayed inverted below it. Only one sharp band at 1792 cm^{-1} appears in the vicinity of the calculated CO stretch (red ν_{CO} in Figure 4a). This is indeed higher than the 1720 cm^{-1} value reported for neutral 1-naphthylbenzoate (**3**),[31] as anticipated for the case of protonation at the ether position. Consistent with the solution phase FTIR measurements, the ν_{CO} transition occurs at a higher frequency than one would expect for a typical isolated carbonyl (i.e., both solvated **1a·H$^+$** ν_{CO} = 1771 cm^{-1} and gas phase ν_{CO} = 1792 cm^{-1} are blue-shifted relative to neutral **1a** ν_{CO} at 1735 cm^{-1}). This effect is predicted at the harmonic level and indeed *opposite* to the situation observed when protonation occurs directly to the carbonyl group. Table 1 summarizes the positions of carbonyl resonances in both solution phase FTIR and cryogenic ion spectra.

The remaining spectroscopic issue involves identifying features arising from the donor NH group on the amine in

dx.doi.org/10.1021/jp211688v | J. Phys. Chem. A 2012, 116, 3556−3560

1a·H$^+$. Solution phase IR of **1a·HB(C$_6$F$_5$)$_4$** reveals a weak, broad peak centered at 3157 cm^{-1}, about 191 cm^{-1} below the value found in the isolated protonated amine. Although it is typical for bands directly involving displacement of hydrogen atoms in charged H-bonds to be dramatically broadened in solution,[32] the gas phase spectra of cold A:H$^+$:B systems have appeared much simpler.[33] It is therefore surprising that the cryogenic **1a·H$^+$** spectrum exhibits a very complex network of strong bands spanning 2700−3200 cm^{-1}, a range that brackets the predicted NH fundamental (ν_{NH}) at 3035 cm^{-1}. Note that the CH stretches also occur in this region but are calculated to be much weaker than the NH fundamental, with less than 5% of the NH stretch intensity. The onset of this broad NH region appears about 500 cm^{-1} below the free NH stretch in **4·H$^+$** (Figure 4b, blue trace) and thus provides clear evidence for an intramolecular hydrogen bond with the NH group. The magnitude of this red shift is anticipated by the large proton affinity difference one would expect between the amine and the atypical ether−ester position.[33] It is interesting to speculate that the unusual complexity associated with the bridging hydrogen in the **1a·H$^+$** spectrum arises because protonation at the ether position significantly weakens the C−O bond to the carbonyl. As such, it is likely that driving vibrational amplitude into the bridging proton motion will strongly couple to this incipient reaction coordinate, which leads to the acylium ion production when gas phase esters are protonated at the ether position. This subject warrants further study, most importantly determining the band evolution upon H/D exchange in the bridging position, but the basic case for an intramolecular NH−O$_{ether}$ H-bond in **1a·H$^+$** is substantiated by the gas phase spectra.

EXPERIMENTAL SECTION

General Methods and Synthesis. See Supporting Information.

Cryogenic Ion Photofragmentation Spectroscopy. The Yale tandem time-of-flight photofragmentation mass spectrometer[34] fitted with a cryogenic, quadropole ion trap[35] was used to synthesize and interrogate cold isolated gas phase ions of protonated compound **1a**. A solution of **1a**, dissolved in HPLC grade acetonitrile doped with ∼1% aqueous formic acid, was electrosprayed into a stainless steel capilary at 25 °C through a PicoTip emitter (15 μm diameter, NewObjective) held at 1.5−2.5 kV potential. Ions were guided by RF only quadrupoles and octopoles through differentially pumped vacuum regions (1, 0.2, 10^{-4}, and 10^{-7} Torr) before reaching the cryogenic 3D ion trap (Jordan, Grass Valley, CA, USA), which was cooled to ∼10 K via a closed-cycle helium cryostat (Janis Research, Wilmington, MA, USA). Pulsing an 80:20 (He/D$_2$) gas mixture at 10 psi for 1 ms through a valve (Parker Hannifin, Series 99) was critical in achieving collision-induced cooling of the ions, which made D$_2$ tagging possible. These van der Waals complexes were ejected from the trap into a Wiley−McLaren time-of-flight extraction region, which was used to separate and isolate ions of different masses before probing them spectroscopically.

The tagged adducts of **1a·H$^+$** were both temporally and spatially focused to intersect with a pulsed infrared laser tunable from 2400 to 4400 cm^{-1} (LaserVision OPO/OPA). To produce radiation in the 600−2400 cm^{-1} range, the OPA idler beam (∼3 μm) was recombined with the signal beam (∼1.5 μm) for difference frequency generation in a AgGaSe$_2$ crystal. The photodissociation of the tagged **1a·H$^+$** and **3·H$^+$** species is described by eq 1.

$$(\mathbf{1a}\cdot\mathbf{H}^+/\mathbf{3}\cdot\mathbf{H}^+)\cdot D_2 + h\upsilon \rightarrow \mathbf{1a}\cdot\mathbf{H}^+/\mathbf{3}\cdot\mathbf{H}^+ + D_2 \quad (1)$$

Using a secondary mass spectrometer, the signal from the **1a·H$^+$** photofragments was detected as a function of photon energy to give the D$_2$ predissociation spectrum. This raw spectrum was normalized to laser energy fluence to correct for differences in laser power throughout the scanned range.

Computational Methods. The Gaussian09 suite of programs[36] was used for all calculations. Density functional theory at the scaled B3LYP/6-311++G** level was implemented to predict the infrared spectrum of compounds **1a·H$^+$** and **3·H$^+$**. The computed spectrum (Figure 1a) was empirically scaled[37] for N−H (0.945) and C−H (0.961) vibrations using the spectrum previously reported for protonated *N*,*N*-dimethylnaphthalen-1-amine[17] (Figure 1b, blue structure), and the carbonyl C═O stretch was scaled by 0.982, based on the experimental value for the C═O stretch in the gas phase benzoic acid monomer.[38] All other vibrations were left unscaled in the fingerprint region. The absorption strengths in km·mol^{-1} were divided by the frequency of the absorbance before normalizing the calculated spectrum so that these intensities could be compared with those experimentally measured. This is necessary because the calculated integrated absorption coefficients are in km·mol^{-1}, which are effectively cross-sections, while the experimental action spectra are normalized to laser energy per pulse. The frequency correction is required to convert this energy to the photon flux.

ASSOCIATED CONTENT

Supporting Information

General experimental methods, synthetic procedures, compound characterization and spectra, and representative solution phase and gas phase IR spectra. This material is available free of charge via the Internet at http://pubs.acs.org.

AUTHOR INFORMATION

Corresponding Author

*E-mail: mark.johnson@yale.edu (M.A.J.); lectka@jhu.edu (T.L.).

Notes

The authors declare no competing financial interest.

ACKNOWLEDGMENTS

M.T.S. thanks JHU for a Marks Graduate Fellowship. T.L. thanks Professors G. J. Meyer and J. P. Toscano for use of their IR spectrometers. M.A.J. would like to thank the NSF (grant CHE-091199) and the Air Force Office of Scientific Research (grant FA-9550-09-1-0139) for funding the cryogenic ESI spectrometer. We thank Lauren A. Martini from the Crabtree lab, who generously provided the chemicals, lab space, and synthesis advice necessary to make 1-naphthylbenzoate. We also thank Arron B. Wolk, Christopher M. Leavitt, Michael Z. Kamrath, and Etienne Garand, whose expertise with this new instrument facilitated data acquisition. Furthermore, we acknowledge the Yale University Faculty of Arts and Sciences High Performance Computing facility, which made all DFT calculations possible.

REFERENCES

(1) Dharmalingam, K.; Ramachandran, K.; Sivagurunathan, P. *Spectrochim. Acta, Part A* **2007**, *66*, 48−51.
(2) Lewis, R. N. A. H.; McElhaney, R. N. *Chem. Phys. Lipids* **1998**, *96*, 9−21.
(3) Huczynski, A.; Rutkowski, J.; Brzezinski, B. *Struct. Chem.* **2011**, *22*, 627−634.
(4) Yeagle, P. L.; Martin, R. B. *Biochem. Biophys. Res. Commun.* **1976**, *69*, 775−780.
(5) Otto, K. E.; Hesse, S.; Wassermann, T. N.; Rice, C. A.; Suhm, M. A.; Stafforst, T.; Diederichsen, U. *Phys. Chem. Chem. Phys.* **2011**, *13*, 14119−14130.
(6) Searles, S.; Tamres, M.; Barrow, G. M. *J. Am. Chem. Soc.* **1953**, *75*, 71−73.
(7) Besseau, F.; Laurence, C.; Berthelot, M. *J. Chem. Soc., Perkin Trans. 2* **1994**, 485−489.
(8) Hansen, P. E.; Christoffersen, M.; Bolvig, S. *Magn. Reson. Chem.* **1993**, *31*, 893−902.
(9) Porte, A. L.; Gutowsky, H. S.; Hunsberger, I. M. *J. Am. Chem. Soc.* **1960**, *82*, 5057−5063.
(10) Yoshimi, Y.; Maeda, H.; Sugimoto, A.; Mizuno, K. *Tetrahedron Lett.* **2001**, *42*, 2341−2343.
(11) Crimmins, M. T.; Choy, A. L. *J. Am. Chem. Soc.* **1997**, *119*, 10237−10238.
(12) Benoit, F. M.; Harrison, A. G. *Org. Mass Spectrom.* **1978**, *13*, 128−132.
(13) Palinko, I. *Acta Crystallogr., Sect. C: Cryst. Struct. Commun.* **2009**, *60*, O642−O643.
(14) Hopkins, A. C.; Csizmadi, I. G. *Theor. Chim. Acta* **1973**, *31*, 83−89.
(15) McClelland, R. A. *J. Am. Chem. Soc.* **1975**, *97*, 3177−3181.
(16) Cox, C.; Wack, H.; Lectka, T. *Angew. Chem., Int. Ed.* **1999**, *38*, 798−800.
(17) Scerba, M. T.; Leavitt, C. M.; Diener, M. E.; DeBlase, A. F.; Guasco, T. L.; Siegler, M. A.; Bair, N.; Johnson, M. A.; Lectka, T. *J. Org. Chem.* **2011**, *76*, 7975−7984.
(18) Bohme, D. K. *Int. J. Mass Spectrom.* **2000**, *200*, 97−136.
(19) Mackay, G. I.; Hopkinson, A. C.; Bohme, D. K. *J. Am. Chem. Soc.* **1978**, *100*, 7460−7464.
(20) Sekiguchi, O.; Bakken, V.; Uggerud, E. *J. Am. Soc. Mass. Spectrom.* **2004**, *15*, 982−988.
(21) Hopkinson, A. C.; Mackay, G. I.; Bohme, D. K. *Can. J. Chem.* **1979**, *57*, 2996−3004.
(22) Tu, Y. P.; Huang, Y. Y.; Atsriku, C.; You, Y.; Cunniff, J. *Rapid Commun. Mass Spectrom.* **2009**, *23*, 1970−1976.
(23) Hu, N.; Tu, Y. P.; Liu, Y. Q.; Jiang, K. Z.; Pan, Y. J. *J. Org. Chem.* **2008**, *73*, 3369−3376.
(24) Yates, K. *Acc. Chem. Res.* **1971**, *4*, 136−144.
(25) Kamrath, M. Z.; Relph, R. A.; Guasco, T. L.; Leavitt, C. M.; Johnson, M. A. *Int. J. Mass Spectrom.* **2010**, *300*, 91−98.
(26) Yeh, L. I.; Okumura, M.; Myers, J. D.; Price, J. M.; Lee, Y. T. *J. Chem. Phys.* **1989**, *91*, 7319−7330.
(27) Hammer, N. I.; Diken, E. G.; Roscioli, J. R.; Johnson, M. A.; Myshakin, E. M.; Jordan, K. D.; McCoy, A. B.; Huang, X.; Bowman, J. M.; Carter, S. *J. Chem. Phys.* **2005**, *122*, 244301.
(28) Gardenier, G. H.; Roscioli, J. R.; Johnson, M. A. *J. Phys. Chem. A* **2008**, *112*, 12022−12026.
(29) Kamrath, M. Z.; Garand, E.; Jordan, P. A.; Leavitt, C. M.; Wolk, A. B.; Van Stipdonk, M. J.; Miller, S. J.; Johnson, M. A. *J. Am. Chem. Soc.* **2011**, *133*, 6440−6448.
(30) Douberly, G. E.; Ricks, A. M.; Ticknor, B. W.; Duncan, M. A. *Phys. Chem. Chem. Phys.* **2008**, *10*, 77−79.
(31) Course, D. J.; Hurlbut, S. L.; Wheeler, D. M. S. *J. Org. Chem.* **1981**, *46*, 374−378.
(32) (a) Stoyanov, E. S. *Phys. Chem. Chem. Phys.* **2000**, *2*, 1137. (b) Stoyanov, E. S.; Reed, C. A. *J. Phys. Chem. A* **110**, *48*, 12992. (c) Asmis, K. R.; Pivonka, N. L.; Santambrogio, G.; Brümmer, M.; Kaposta, C.; Neumark, D. M.; Wöste, L. *Science* **2003**, *299*, 1375−1377. (d) Moore, D. T.; Oomens, J.; van der Meer, L.; von Helden, G.; Meijer, G.; Valle, J.; Marshall, A. G.; Eyler, J. R. *ChemPhysChem* **2004**, *5*, 740−743. (e) Fridgen, T. D.; MacAleese, L.; Maitre, P.; McMahon, T. B.; Boissel, P.; Lemaire, J. *Phys. Chem. Chem. Phys.* **2005**, *7*, 2747. (f) Ault, B. S.; Steinback, E.; Pimentel, G. C. *J. Phys. Chem.* **1975**, *79*, 615−620. (g) Zundel, G. *Adv. Chem. Phys.* **2000**, *111*, 1−217. (h) Novak, A. *Struct. Bonding* **1974**, *18*, 177−216. (i) Nizkorodov, S. A.; Dopfer, O.; Meuwly, M.; Maier, J. P.; Bieske, E. J. *J. Chem. Phys.* **1996**, *105*, 1770−1777.
(33) Roscioli, J. R.; McCunn, L. R.; Johnson, M. A. *Science* **2007**, *316*, 249−254.
(34) Johnson, M. A.; Lineberger, W. C. In *Techniques for the Study of Ion−Molecule Reactions*; Farrar, J. M., Saunders, W. H., Jr., Eds.; Wiley: New York, 1988; Vol. *20*, p 591.
(35) Kamrath, M. Z.; Relph, R. A.; Guasco, T. L.; Leavitt, C. M.; Johnson, M. A. *Int. J. Mass Spectrom.* **2011**, *300*, 91−98.
(36) Frisch, M. J.; Trucks, G. W.; Schlegel, H. B.; Scuseria, G. E.; Robb, M. A.; Cheeseman, J. R.; Scalmani, G.; Barone, V.; Mennucci, B.; Petersson, G. A.; Nakatsuji, H.; Caricato, M.; Li, X.; Hratchian, H. P.; Izmaylov, A. F.; Bloino, J.; Zheng, G.; Sonnenberg, J. L.; Hada, M.; Ehara, M.; Toyota, K.; Fukuda, R.; Hasegawa, J.; Ishida, M.; Nakajima, T.; Honda, Y.; Kitao, O.; Nakai, H.; Vreven, T.; Montgomery, J. A., Jr.; Peralta, J. E.; Ogliaro, F.; Bearpark, M.; Heyd, J. J.; Brothers, E.; Kudin, K. N.; Staroverov, V. N.; Kobayashi, R.; Normand, J.; Raghavachari, K.; Rendell, A.; Burant, J. C.; Iyengar, S. S.; Tomasi, J.; Cossi, M.; Rega, N.; Millam, J. M.; Klene, M.; Knox, J. E.; Cross, J. B.; Bakken, V.; Adamo, C.; Jaramillo, J.; Gomperts, R.; Stratmann, R. E.; Yazyev, O.; Austin, A. J.; Cammi, R.; Pomelli, C.; Ochterski, J. W.; Martin, R. L.; Morokuma, K.; Zakrzewski, V. G.; Voth, G. A.; Salvador, P.; Dannenberg, J. J.; Dapprich, S.; Daniels, A. D.; Farkas, O.; Foresman, J. B.; Ortiz, J. V.; Cioslowski, J.; Fox, D. J. *Gaussian 09*, revision x.x; Gaussian, Inc.: Wallingford, CT, 2009.
(37) Temelso, B.; Shields, G. C. *J. Chem. Theory Comput.* **2011**, *7*, 2804−2817.
(38) Bakker, J. M.; Mac Aleese, L.; von Helden, G.; Meijer, G. *J. Chem. Phys.* **2003**, *119*, 11180−11185.